Supplementary File

Nickel-Iron Alloy Nanoparticle-Modified Carbon Fibre and Nickel-Coated Carbon Fibre Catalyst Materials for Hydrogen and Oxygen Evolution Reactions in 0.1 M NaOH Solution

Mateusz Kuczyński, Tomasz Mikołajczyk*, Bogusław Pierożyński

Department of Chemistry, Faculty of Agriculture and Forestry, University of Warmia and Mazury in Olsztyn, Łódzki Square 4, 10-727 Olsztyn, Poland

*Corresponding author: Tomasz Mikołajczyk; Phone: +48 89 523-4177; Fax: +48 89 523-4801; E-mail address: tomasz.mikolajczyk@uwm.edu.pl;

Abstract

This study presents the results of electrochemical investigations on Hydrogen and Oxygen Evolution Reactions (HER and OER), conducted on commercially available carbon fibres and nickel-coated carbon fibres modified with nanoscale NiFe alloy particles in 0.1 M NaOH solution. The obtained results demonstrated enhanced catalytic activity of the NiFe-modified fibre materials, with approximately 14,700% and 25% improvement in the OER and HER activity (respectively), as compared to unmodified electrodes. The catalytic properties were evaluated by means of electrochemical impedance spectroscopy, Tafel polarisation and cyclic, and linear voltammetry techniques. The deposited particles' distribution and quantities present on the investigated materials were analysed using Scanning Electron Microscopy (SEM) and Energy-Dispersive X-Ray spectroscopy (EDX) methods. These findings provided valuable insights into electrochemical, catalytic performance of NiFe-modified carbon fibre/nickel-coated carbon fibre materials, simultaneously highlighting their potential application as catalyst materials for electrodes in industrial-scale water electrolysers.

The purpose of this supplementary file is to provide additional data, analyses and methodological details that complement the findings presented in the main manuscript. Expanded data sets include cyclic voltammetry and impedance measurements, particularly those normalized to electrochemically active surface area (ECSA).

To accurately determine the ECSA of all electrodes, we utilized potential sweep measurements to calculate the double-layer capacitance. These sweeps were conducted at a potential centred around 0.7 V vs. RHE, within a range of ± 0.10 V of this central potential. The sweep-rates for these measurements varied between 5 and 100 mV/s.

Calculation of Differential Capacitance

For the calculation of the differential capacitance C_{DL}, two basic equations are employed:

$$C_{DL} = \frac{DQ}{D\varphi} \qquad \text{Equation (1)}$$

$$i = \frac{dQ(\varphi)}{dt} \qquad \text{Equation (2)}$$

Here, C_{DL} represents the double-layer capacitance, Q is the charge, φ is the potential, and *i* is the current.

From Equations (1) and (2), the following relationship is derived:

$$i = C_{DL}\frac{d\varphi}{dt} \qquad \text{Equation (3)}$$

The calculated current densities as a function of the scan rate demonstrated linear behaviour over the measured range (see Figure S1) [1].

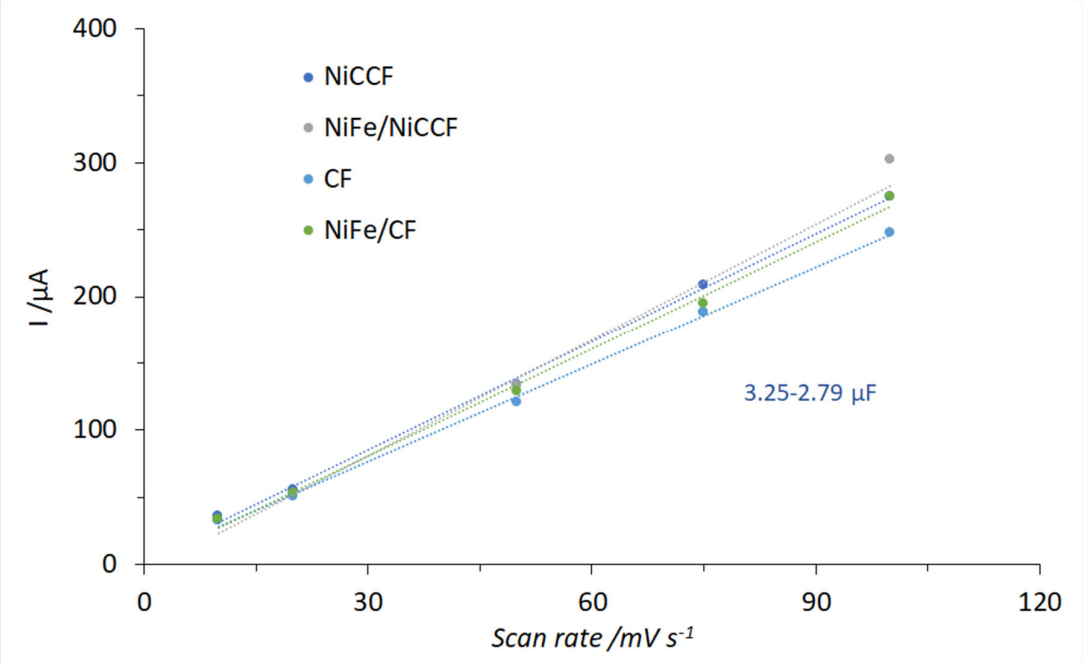

Figure S1. Average current densities measured at the potential of 0.7 V vs. RHE, plotted as a function of scan rate. The slope of the linear fit gives the double-layer capacitance.

The average ECSA of all electrodes was estimated to be approximately 0.15 cm^2 based on the double-layer capacitance measurements, in reference to that commonly used value of 20 µF cm^{-2} in literature for smooth and homogeneous surfaces [2]. The electrochemical parameters presented in this supplementary file were calculated using this average ECSA.

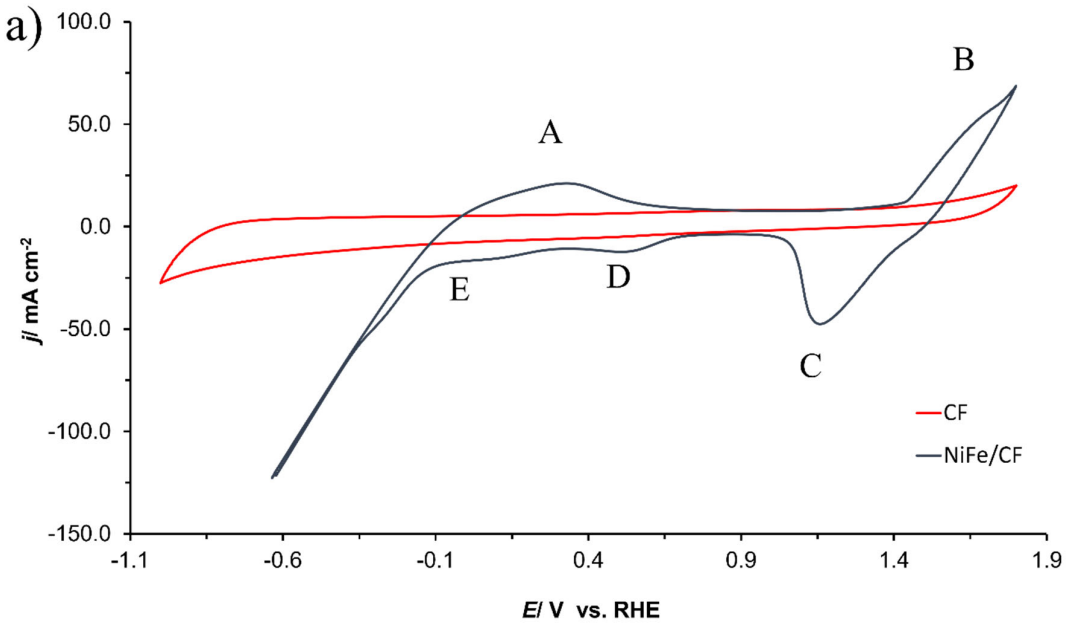

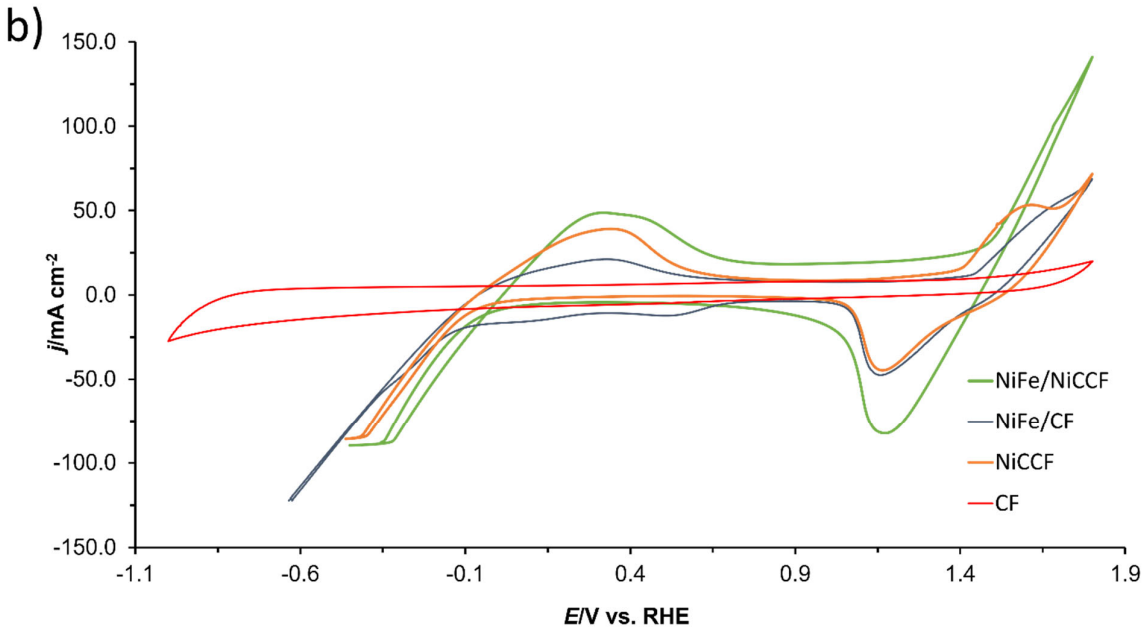

Figure S2. Cyclic voltammogram curves of (a) CF and NiFe/CF; (b) CF, NiCCF, NiFe/CF and NiFe/NiCCF electrodes in contact with 0.1 M NaOH medium, carried-out at a scan-rate of 50 mV s^{-1} for the potential span from -1.0 to 1.8 V vs. RHE.

The current densities in the main manuscript based on the geometrical surface area (GSA), which came to ca. -0.5 and 0.3 mA/cm^2 at -0.6 and 1.8 V vs RHE, respectively, for NiFe/CF catalyst compared to existing literature [3] values of *ca*. -15 and 15 mA/cm^2 for similar potentials are notably smaller. This discrepancy stems from our initial reliance on the manufacturer-provided surface areas for both CF and NiCCF materials. However, the electrochemically active surface area (ECSA) was found to be approximately 300 times smaller, and it was observed that the parameters based on the ECSA seemed overly optimistic, reaching values of -125 and 75 mA/cm^2 for NiFe/CF electrode at the corresponding potentials. Additionally, the unmodified CF reached a value of about -16 mA/cm^2, which also causes some dissonance with the results available in the literature.

Table S1. Current densities for HER (η= 0.35 V) and OER (η= 0.57 V) recorded from CV curves.

Sample	Current densities [mA cm^{-2}]	
	HER $_{\eta= 0.35\ V}$	OER $_{\eta= 0.57\ V}$
CF	-10.9	20.0
NiFe/CF	-57.7	68.6
NiCCF	-72.5	72.8
NiFe/NiCCF	-88.6	142.8

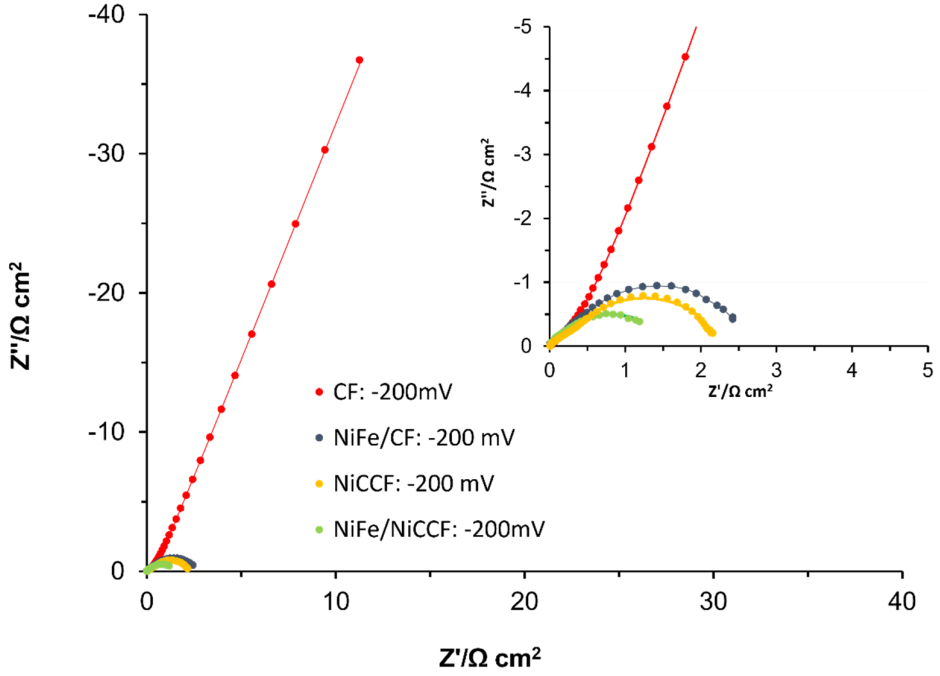

Figure S3. Electrochemical impedance Nyquist plots for the HER on CF, NiCCF, NiFe/CF and NiFe/NiCCF electrode surfaces in contact with 0.1 M NaOH (at 293K) for the potential of -200 mV vs. RHE.

Table S2. Exchange current densities for the HER (calculated based on the Butler-Volmer equation) in 0.1 M NaOH.

Material	HER	
	j_0 [A cm^{-2}]	Ref.
CF	4.7×10^{-9}	This work
NiFe/CF	4.4×10^{-4}	This work
NiCCF	4.0×10^{-4}	This work
NiFe/NiCCF	4.8×10^{-4}	This work
Ru/NiCCF	5.4×10^{-5}	[4]
Pd/CF	1.7×10^{-5}	[5]
Ru/CF	7.7×10^{-6}	[6]

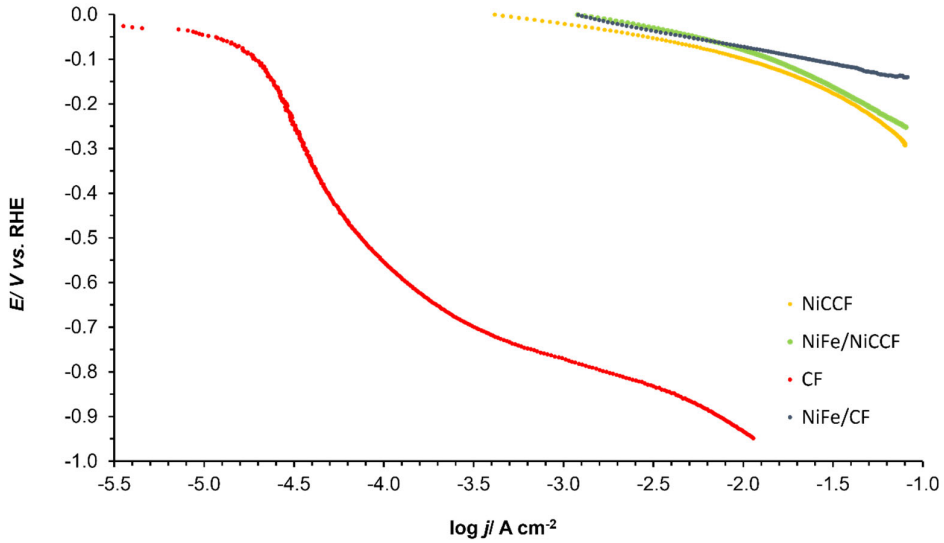

Figure S4. Quasi-potentiostatic cathodic polarisation curves for the hydrogen evolution reaction (HER), obtained at CF, NiFe/CF, NiCCF, and NiFe/NiCCF electrodes in 0.1 M NaOH electrolyte. The polarisation curves were recorded at a scan rate of 0.5 mV s^{-1}. The impedance-based solution resistance, i*R* correction was also applied.

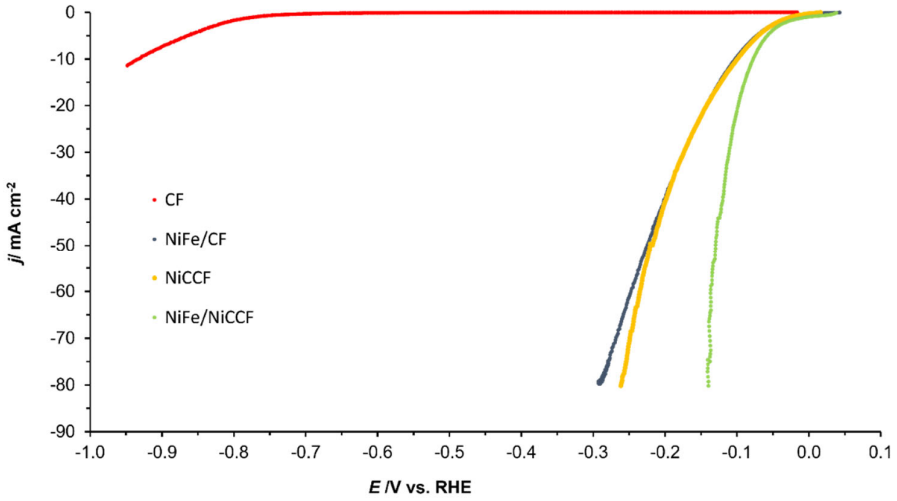

Figure S5. Linear Sweep Voltammetry (LSV) curves of CF, NiFe/CF, NiCCF and NiFe/NiCCF electrodes in 0.1 M NaOH solution, carried out with a scan rate of 0.5 mV s^{-1} for the HER.

Table S3. HER kinetic parameters for the selected catalytic materials.

Material	b_c [mV dec^{-1}]	j_0 [A cm^{-2}]	Ref.	Electrolyte
CF	-108	8.1×10^{-11}	This work	0.1 M NaOH
NiFe/CF	-62	4.4×10^{-4}	This work	0.1 M NaOH
NiCCF	-63	4.3×10^{-4}	This work	0.1 M NaOH
NiFe/NiCCF	-67	3.4×10^{-4}	This work	0.1 M NaOH

NiFe/NiFoam	157	1.7×10^{-5}	[7]	1.0 M KOH
Ni	-	2.3×10^{-6}	[8]	0.1 M NaOH
Pt	-150	1.0×10^{-5}	[9]	0.1 M NaOH
NiSn/Cu	-121	6.9×10^{-7}	[3]	1.0 M KOH
NiCoSn/Cu	-122	1.2×10^{-5}	[3]	1.0 M KOH
NiCu/C	-57	2.5×10^{-5}	[10]	1.0 M KOH

The ECSA-normalized values for HER performance (Tables S2 and S3) were significantly higher than those for conventional nickel [8] and even platinum [9] electrodes. While this could potentially poInt. to an exceptionally high density of active sites, these results appeared somewhat overly optimistic.

To provide a more balanced and rigorous assessment, we decided to adopt a dual approach by reporting electrochemical parameters based on the geometrical surface area (GSA) in the main manuscript and the ECSA in the supplementary file. This methodology allows us to present a more comprehensive view of the electrochemical performance of our NiFe/CF and NiFe/NiCCF electrodes. Using GSA as a basis offers a conservative comparison with established materials, such as nickel and platinum, while the ECSA-based parameters highlight the potential for optimization and the intrinsic activity of our modified electrodes.

By employing this dual approach, we aim to facilitate a more subtle interpretation of our results and to allow for more robust comparisons with other studies in the field of HER catalysis.

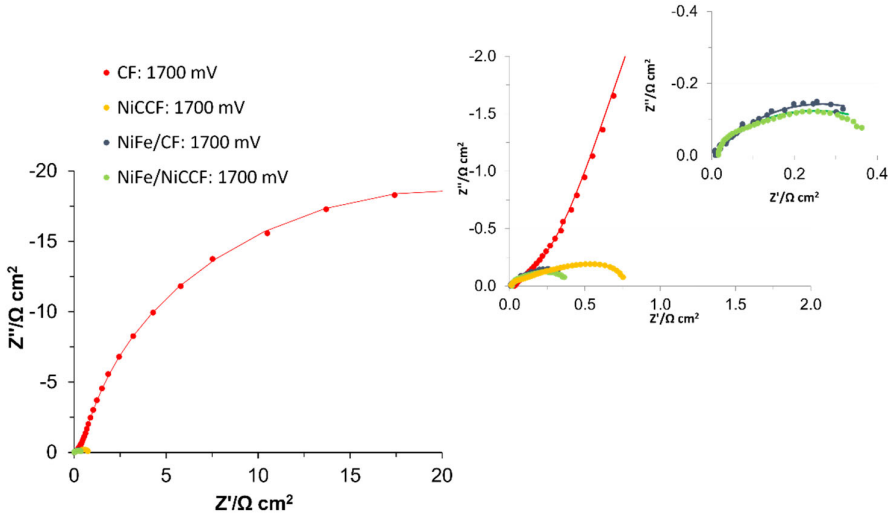

Figure S6. Electrochemical Nyquist impedance plots for the OER on CF, NiCCF, NiFe/CF and NiFe/NiCCF electrode surfaces in contact with 0.1 M NaOH solution (at 293K) for the potential of 1700 mV vs. RHE.

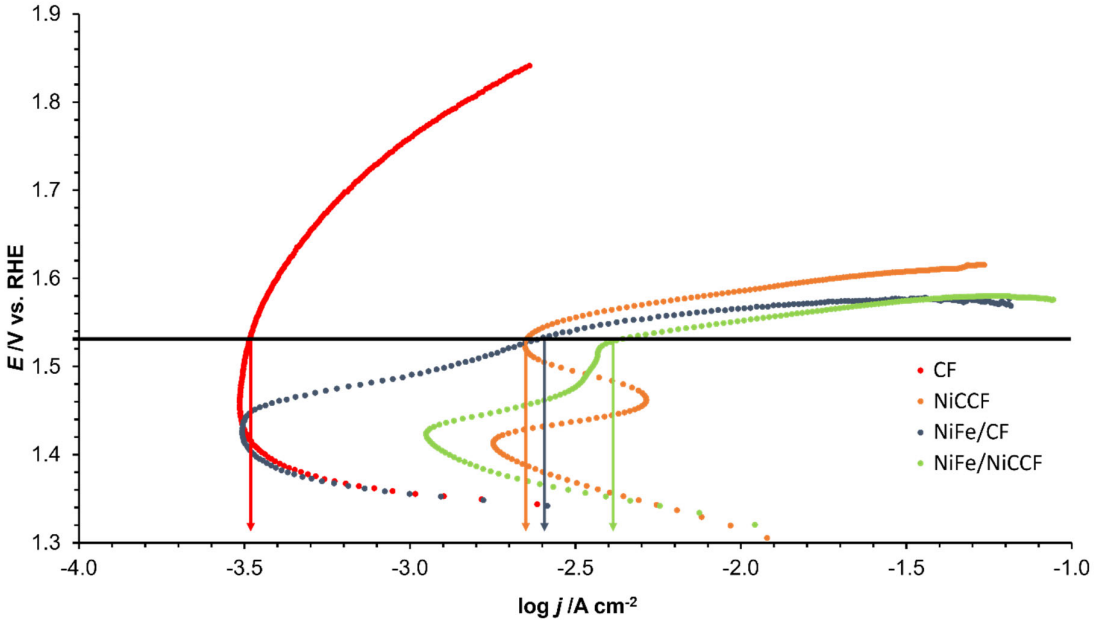

Figure S7. Quasi-potentiostatic cathodic polarisation curves for the oxygen evolution reaction (OER) obtained for CF, NiFe/CF, NiCCF and NiFe/NiCCF electrodes in 0.1 M NaOH solution. The polarisation curves were recorded at a scan rate of 0.5 mV s^{-1}. The black line represents the overpotential of 300 mV. Arrows on the graph show the logarithm of the current density (log *j*) for each sample; the colour of the arrow matches the colour of the corresponding sample plot. The i*R* correction was applied to account for the solution resistance, based on the impedance measurements.

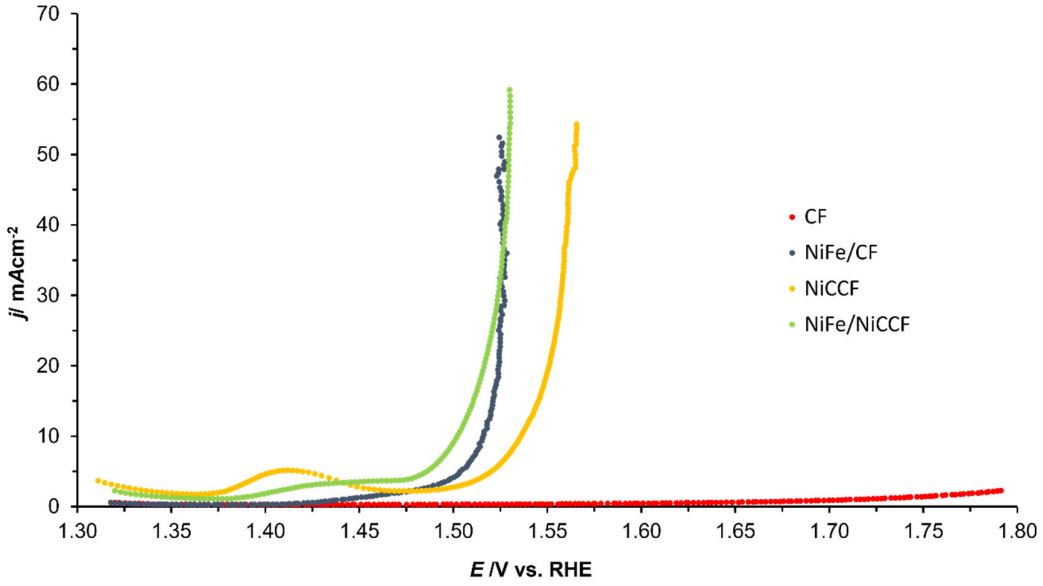

Figure S8. Linear Sweep Voltammetry (LSV) curves of CF, NiFe/CF, NiCCF and NiFe/NiCCF electrodes in 0.1 M NaOH solution, carried-out with a scan rate of 0.5 mV s^{-1} for the OER.

Table S4. OER kinetic parameters for the selected catalytic materials.

Material	Electrolyte	b_a [mV dec^{-1}]	$j_{(\eta=0.3\ V)}$ [A cm^{-2}]	$\eta_{(j=10\ mA\ cm^{-2})}$ [mV]	Ref.
CF	0.1 M NaOH	261	2.5×10^{-3}	560	This work
NiFe/CF	0.1 M NaOH	40	2.4×10^{-2}	290	This work
NiCCF	0.1 M NaOH	74	1.1×10^{-2}	305	This work
NiFe/NiCCF	0.1 M NaOH	60	4.9×10^{-2}	270	This work
RuO_2/GC	0.1 M NaOH	44	~5.0×10^{-4}	-	[11]
Co_3O_4/GC	0.1 M KOH	69	5.9×10^{-6}	-	[12]
$CoAl_2O_4$/GC	0.1 M KOH	56	3.9×10^{-7}	-	[12]
$ZnCo_2O_4$/GC	0.1 M KOH	113	5.6×10^{-7}	-	[12]
Pt	1.0 M KOH	66	4.0×10^{-4}	-	[13]
Ni/Fe	1.0 M NaOH	38	3.3×10^{-5}	-	[14]
Co/Fe	1.0 M NaOH	46	1.2×10^{-5}	-	[14]
IrO_2/GC	1.0 M KOH	76	3.9×10^{-3}	-	[15]
CoP/C	1.0 M KOH	71	5.0×10^{-3}	-	[15]
NiFe-LDH/GC	1.0 M KOH	35	~9.0×10^{-4}	320	[16]
$Ni_{0.25}Co_{0.75}O_x$	1.0 M KOH	36	7.9×10^{-5}	377	[17]
NiCo-LDH/GC	1.0 M KOH	41	-	335	[18]
$MnFe_2O_4$/GC	0.1 M KOH	114	-	470	[19]
$NiFe_2O_4$/GC	0.1 M KOH	98	-	440	[19]

The current density values recorded on the examined materials at an anodic overpotential of 300 mV were superior to those achieved by bulk NiFe-LDH (Layered Double Hydroxide) materials [18]. Moreover, the NiFe-modified CF and NiCCF electrodes exhibited higher current densities than certain other catalytic materials, such as IrO_2 or CoP.

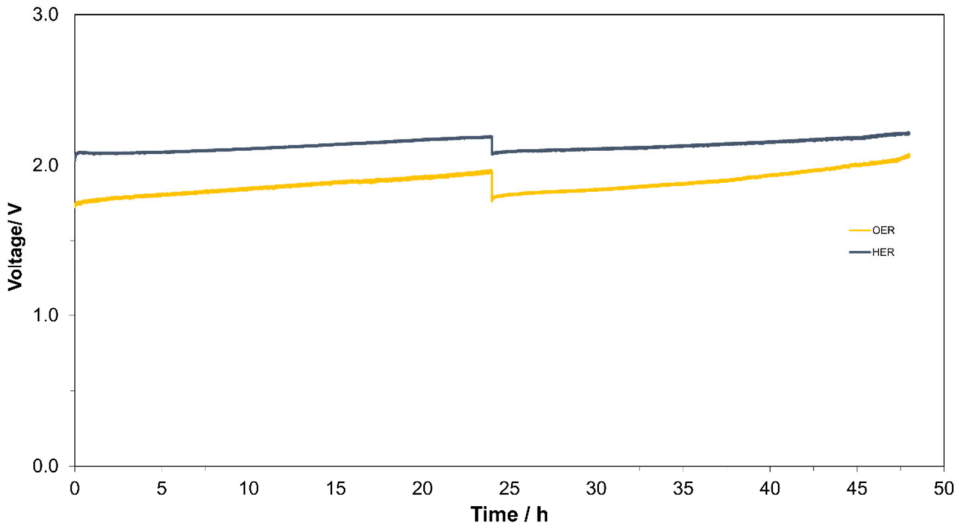

Figure S9. Long-term electrochemical stability tests of NiFe alloy on the CF were conducted at a current density of 15 mA cm^{-2}. The system consisted of a NiFe/CF working electrode and a Ti/Pt counter electrode.

Table S5. Composition of electrodeposition baths and process parameters to prepare *ca.* 10 wt. % of NiFe alloy deposits

Reagents	**Concentration (M)**	**Process parameters**
$NiSO_4 \times 6\ H_2O$ (9.0%, Sigma Aldrich, SaInt. Louis, USA)	0.48	Anode: Pt foil Cathode: CF/NiCCF Temperature: 313 K Deposition time: 15 s Current-density: 1 mA cm^{-2} Solution pH: 3.0
$NiCl_2 \times 6\ H_2O$ (98%, POCH, Gliwice, Poland)	0.58	
H_3BO_3 (>99.5%, POCH, Gliwice, Poland)	0.73	
$FeSO_4 \times 7\ H_2O$ (99%, AKTYN, Suchy Las, Poland)	0.07	

References

1. Connor P, Schuch J, Kaiser B, Jaegermann W. The Determination of Electrochemical Active Surface Area and Specific Capacity Revisited for the System MnO_x as an Oxygen Evolution Catalyst. *Z Für Phys Chem* **2020**, *234*, 979–994. https://doi.org/10.1515/zpch-2019-1514.
2. Lasia A. Mechanism and kinetics of the hydrogen evolution reaction. *Int. J. Hydrog. Energy* **2019**, *44*, 19484–19518. https://doi.org/10.1016/j.ijhydene.2019.05.183.
3. Vijayakumar J, Mohan S, Anand Kumar S, Suseendiran SR, Pavithra S. Electrodeposition of Ni–Co–Sn alloy from choline chloride-based deep eutectic solvent and characterization as cathode for hydrogen evolution in alkaline solution. *Int. J. Hydrog. Energy* **2013** *38*, 10208–10214. https://doi.org/10.1016/j.ijhydene.2013.06.068.

4. Pierożyński B, Mikołajczyk T. Hydrogen evolution reaction at Ru-modified nickel-coated carbon fibre in 0.1 M NaOH. *Pol. J. Chem. Technol.* **2015**, *17*, 18–22. https://doi.org/10.1515/pjct-2015-0004.
5. Pierozynski B, Mikolajczyk T, Turemko M, Czerwosz E, Kozlowski M. Hydrogen evolution reaction at Pd-modified carbon fibre in 0.1 M NaOH. *Int. J. Hydrog. Energy* **2015**, *40*, 1795–1799. https://doi.org/10.1016/j.ijhydene.2014.12.029.
6. Mikolajczyk T, Pierozynski B. Influence of Electrochemical Oxidation of Carbon Fibre on Cathodic Evolution of Hydrogen at Ru-Modified Carbon Fibre Material Studied in 0.1 M NaOH. *Int. J. Electrochem. Sci.* **2013**, *8*.
7. Wang M, Wang J-Q, Xi C, Cheng C-Q, Kuai C-G, Zheng X-L, et al. Valence-State Effect of Iridium Dopant in NiFe(OH)2 Catalyst for Hydrogen Evolution Reaction. *Small* **2021**, *17*, 2100203. https://doi.org/10.1002/smll.202100203.
8. Zhou Z, Liu Y, Zhang J, Pang H, Zhu G. Non-precious nickel-based catalysts for hydrogen oxidation reaction in alkaline electrolyte. *Electrochem. Commun.* **2020**, *121*, 106871. https://doi.org/10.1016/j.elecom.2020.106871.
9. Zheng Y, Jiao Y, Vasileff A, Qiao S-Z. The Hydrogen Evolution Reaction in Alkaline Solution: From Theory, Single Crystal Models, to Practical Electrocatalysts. *Angew. Chem. Int. Ed.* **2018**, *57* 7568–7579. https://doi.org/10.1002/anie.201710556.
10. Gao MY, Yang C, Zhang QB, Yu YW, Hua YX, Li Y, et al. Electrochemical fabrication of porous Ni-Cu alloy nanosheets with high catalytic activity for hydrogen evolution. *Electrochimica Acta* **2016**, *215*, 609–616. https://doi.org/10.1016/j.electacta.2016.08.145.
11. Reier T, Oezaslan M, Strasser P. Electrocatalytic Oxygen Evolution Reaction (OER) on Ru, Ir, and Pt Catalysts: A Comparative Study of Nanoparticles and Bulk Materials. *ACS Catal* **2012**, *2*, 1765–1772. https://doi.org/10.1021/cs3003098.
12. Wang H-Y, Hung S-F, Chen H-Y, Chan T-S, Chen HM, Liu B. In Operando Identification of Geometrical-Site-Dependent Water Oxidation Activity of Spinel Co3O4. ACS Publ 2015. https://doi.org/10.1021/jacs.5b10525.
13. Cui X, Zhang B, Zeng C, Guo S. Electrocatalytic activity of high-entropy alloys toward oxygen evolution reaction. *MRS Commun.* **2018**, *8*, 1230–1235. https://doi.org/10.1557/mrc.2018.111.
14. Lyons MEG, Brandon MP. The Oxygen Evolution Reaction on Passive Oxide Covered Transition Metal Electrodes in Alkaline Solution. *Part III – Iron. Int. J Electrochem Sci* **2008**, *3*.
15. Chang J, Xiao Y, Xiao M, Ge J, Liu C, Xing W. Surface Oxidized Cobalt-Phosphide Nanorods As an Advanced Oxygen Evolution Catalyst in Alkaline Solution. *ACS Catal* **2015**, *5*, 6874–6878. https://doi.org/10.1021/acscatal.5b02076.
16. Gong M, Li Y, Wang H, Liang Y, Wu JZ, Zhou J, et al. An Advanced Ni–Fe Layered Double Hydroxide Electrocatalyst for Water Oxidation. *J. Am. Chem. Soc.* **2013**, *135*, 8452–8455. https://doi.org/10.1021/ja4027715.
17. Song F, Hu X. Exfoliation of layered double hydroxides for enhanced oxygen evolution catalysis. *Nat. Commun.* **2014**, *5*, 4477. https://doi.org/10.1038/ncomms5477.
18. Suen N-T, Hung S-F, Quan Q, Zhang N, Xu Y-J, Chen HM. Electrocatalysis for the oxygen evolution reaction: recent development and future perspectives. *Chem. Soc. Rev.* **2017**, *46*, 337–365. https://doi.org/10.1039/C6CS00328A.
19. Li M, Xiong Y, Liu X, Bo X, Zhang Y, Han C, et al. Facile synthesis of electrospun MFe2O4 (M = Co, Ni, Cu, Mn) spinel nanofibers with excellent electrocatalytic properties for oxygen evolution and hydrogen peroxide reduction. *Nanoscale* **2015**, *7*, 8920–8930. https://doi.org/10.1039/C4NR07243J.